Consistent and Elastic Registration of Histological Sections Using Vector-Spline Regularization

Ignacio Arganda-Carreras[1,3], Carlos O.S. Sorzano[1,5], Roberto Marabini[1,3], José María Carazo[1], Carlos Ortiz-de-Solorzano[2], and Jan Kybic[4]

[1] Biocomputing Unit, National Centre of Biotechnology,
Universidad Autónoma de Madrid, 28049 Cantoblanco, Madrid, Spain
{iarganda, coss, roberto, carazo}@cnb.uam.es
http://biocomp.cnb.uam.es/
[2] Cancer Imaging Laboratory, Centre for Applied Medical Research (CIMA),
31008 Pamplona, Spain
codesolorzano@unav.es
http://www.cima.es/index_english.html
[3] Escuela Politécnica Superior, Universidad Autónoma de Madrid,
28049 Madrid, Spain
{Ignacio.Arganda, Roberto.Marabini}@uam.es
http://www.ii.uam.es/esp/welcomii.php?idioma=eng
[4] Center for Machine Perception, Czech Technical University,
121 35 Prague 2, Czech Republic
kybic@fel.cvut.cz
http://cmp.felk.cvut.cz/
[5] Escuela Politécnica Superior, Univ. San Pablo CEU, 28003 Madrid, Spain
coss.eps@ceu.es
http://www.uspceu.com/

Abstract. Here we present a new image registration algorithm for the alignment of histological sections that combines the ideas of B-spline based elastic registration and consistent image registration, to allow simultaneous registration of images in two directions (direct and inverse). In principle, deformations based on B-splines are not invertible. The consistency term overcomes this limitation and allows registration of two images in a completely symmetric way. This extension of the elastic registration method simplifies the search for the optimum deformation and allows registering with no information about landmarks or deformation regularization. This approach can also be used as the first step to solve the problem of group-wise registration. . . .

1 Introduction

Studying the three-dimensional organization of complex histological structures requires imaging, analyzing and registering large sets of images taken from serially sectioned tissue blocks. We have developed an integrated microscopy system that automates or greatly reduces the amount of interaction required for these tasks [1,2] and provides volumetric renderings of the structures in the tissue.

Proper section alignment is the first step towards an accurate 3D tissue reconstruction, as it is in other imaging modalities [3,4]. In our case we perform a coarse alignment of the sections using an automatic rigid-body registration method [5]. This method can not correct some non-linear distorting effects (e.g. tissue folding, stretching, tearing, etc.) caused by the manual sectioning process. Moreover, the distance between sections causes significant differences between the same structures of interest in consecutive sections, which could be misinterpreted by a complete linear registration process. Therefore, a non-linear or local method is strongly needed in order to refine the first registration step.

In this paper we present a new method for elastic and consistent registration of histological sections. All the examples described in the paper used mammary gland tissue samples; however, the same algorithm could be equally applied to other tissue sources and image modalities.

2   Methodology

The properties of B-splines have been largely proved to be very useful when modeling deformations in many biomedical imaging problems; such as tracking the movement of the left ventricle from MRI images [6], reconstructing the 3-D motion of the cardiac cycle [7] or modeling the motion of the breast by dynamic MR imaging [8].

The registration of a source image with a target image can be defined as the problem of finding a deformation field that transforms coordinates of the target image into coordinates of the source image. The main problem of using B-spline deformation fields is that the estimated field might not be invertible (which is not a problem since depending on the specific case, the true deformation field may not be invertible neither). However, in case it were invertible, the inverse deformation field can be computationally expensive. Either it is invertible or not, it is convenient to have also a way of transforming coordinates in the source image into coordinates of the target. This would define a second deformation field that is close to the inverse of the original field and it has proven to be useful as a way of regularizing the registration problem [9,10]. This two-way registration is known as consistent registration. [10] achieves the consistency by forcing the deformation field to be a diffeomorphism (continuous, differentiable, and invertible, its inverse must also be continuous and differentiable). This is a too strong constraint for our images, although it has the advantage of not having to compute two separate fields since the diffeomorphism condition automatically guarantees the existence of the deformation inverse. [9] computes two independent deformations whose composition should be as close as possible to the identity transformation. Thus, one is not the inverse of the other. This closeness to identity is explicitly introduced into the objective function.

In this work we combine the idea of elastic registration using vector-spline regularization [11] with that of a consistent registration [9]. We combine both ideas and extend them in order to overcome their limitations. The standard registration method presented in [11] propose the calculation of the elastic deformation

field trough the minimization of an energy functional composed by three terms: the energy of the similarity error between both images (represented by the pixelwise mean-square distance), the error of the mapping of soft landmarks, and a regularization term based on the divergence and the curl of the deformation to ensure its smoothness. This minimization is optimized by a variant of the robust Levenberg-Marquardt method.

We transform the energy functional presented in [11] into a new functional that incorporates a factor of the deformation field consistency. Unlike in [11], we are now looking for two transformations at the same time (direct and inverse). Therefore, the vectors passed to the Levenberg-Marquardt optimizer are now twice as long. Besides the measurement of dissimilarity between the source and target images (now in both directions) E_{img}, the optional landmark constraint E_μ and the regularization term $(E_{\text{div}} + E_{\text{rot}})$, we add a new energy term E_{cons} that expresses the geometrical consistency between the elastic deformation in one direction (from source to target) and the other direction (from target to source). Therefore, the energy function is now given by

$$E = w_{\text{i}} E_{\text{img}} + w_\mu E_\mu + (w_{\text{d}} E_{\text{div}} + w_{\text{r}} E_{\text{rot}}) + w_{\text{c}} E_{\text{cons}} . \tag{1}$$

Where w_{x} are the specific weights given to the different energy terms.

2.1   Consistency Term

The consistency energy represents the geometrical distances between the pixel coordinates after applying both transformations (direct-inverse or inverse-direct), i.e. the amount by which the composed transformation differs from identity. The standard approach [11] for this type of registration is to find a deformation function

$$g^+(x) : \mathbb{R}^2 \to \mathbb{R}^2 . \tag{2}$$

This function transforms the source image I_{s} into an image as similar as possible to the target image I_{s}. This transformation g^+ maps coordinates in I_{s} into coordinates in I_{t}. Here, following [9], we will also simultaneously look for its corresponding inverse function

$$g^-(x) : \mathbb{R}^2 \to \mathbb{R}^2 . \tag{3}$$

This function maps the coordinates in I_{t} into coordinates in I_{s}.

Following this notation, our consistency energy term is given by

$$
\begin{aligned}
E_{\text{cons}} &= E_{\text{cons}}^+ + E_{\text{cons}}^- \\
&= \int_{\mathbf{x} \in \mathbb{R}^2} \|\mathbf{x} - g^-(g^+(\mathbf{x}))\|^2 \, d\mathbf{x} + \int_{\mathbf{x} \in \mathbb{R}^2} \|\mathbf{x} - g^+(g^-(\mathbf{x}))\|^2 d\mathbf{x} .
\end{aligned} \tag{4}
$$

If we approximate the integrals by discrete sums and restrict the integration domain, we obtain

$$E_{\text{cons}}^+ = \frac{1}{\#\Omega^+} \sum_{\mathbf{x} \in \Omega^+} \|\mathbf{x} - g^-(g^+(\mathbf{x}))\|^2 . \tag{5}$$

$$E_{\text{cons}}^- = \frac{1}{\#\Omega^-} \sum_{\mathbf{x} \in \Omega^-} \|\mathbf{x} - g^+(g^-(\mathbf{x}))\|^2 . \tag{6}$$

Where , Ω^+, Ω^- define sets of relevant pixels common to the target and source images:

$$\Omega^+ = \left\{ \mathbf{x} \in \Omega_s \cap \mathbb{Z}^2 : g^+(\mathbf{x}) \in \Omega_t \cap \mathbb{Z}^2 \right\} . \tag{7}$$

$$\Omega^- = \left\{ \mathbf{x} \in \Omega_t \cap \mathbb{Z}^2 : g^-(\mathbf{x}) \in \Omega_s \cap \mathbb{Z}^2 \right\} . \tag{8}$$

And where $\#\Omega^+$ and $\#\Omega^-$ are the number of pixels in the masks.

2.2 Deformation Representation

Following [11] we represent the deformation fields as a linear combination of B-splines. For instance, g^+:

$$\begin{aligned}
g^+(\mathbf{x}) &= g^+(x, y) \\
&= \left(g_1^+(x, y), g_2^+(x, y) \right) \\
&= \sum_{k.l \in \mathbb{Z}^2} \begin{pmatrix} c_{1,k,l}^+ \\ c_{2,k,l}^+ \end{pmatrix} \beta^3 \left(\frac{x}{s_x} - k \right) \beta^3 \left(\frac{y}{s_y} - l \right) .
\end{aligned} \tag{9}$$

Where β^3 is the B-spline of degree 3, $c_{k,l}$ are the B-spline coefficients, and s_x and s_y are scalars (sampling steps) controlling the degree of detail of the representation of the deformation field.

2.3 Explicit Derivatives

The chosen optimizer uses gradient information. We will now calculate the derivatives of the energy function with respect to all the parameters, starting with E_{cons}. It can be easily shown that the derivative of E_{cons}^+ with respect to any of the deformation coefficients defining the first component (x in our case) of the direct deformation field g^+, is given by

$$\frac{\partial E_{\text{cons}}^+}{\partial c_{1,k,l}^+} = -2 \sum_{\mathbf{x} \in \Omega^+} \left(\mathbf{x} - g^-(g^+(\mathbf{x})) \right) \cdot \left(\frac{\partial}{\partial c_{1,k,l}^+} \left(g^-(g^+(\mathbf{x})) \right) \right) . \tag{10}$$

Where

$$\frac{\partial}{\partial c_{1,k,l}^+} \left(g^-(g^+(\mathbf{x})) \right) = \left(\left. \frac{\partial g_1^-}{\partial x} \right|_{x',y'} , \left. \frac{\partial g_2^-}{\partial y} \right|_{x',y'} \right) \left. \frac{\partial g_1^+}{\partial c_{1,k,l}^+} \right|_{x,y} . \tag{11}$$

And where

$$\mathbf{x} = (x, y) . \tag{12}$$

And

$$(x, y) = g^+(x, y) \ . \tag{13}$$

Again, following the definition of the transformation function we express its derivative with respect to the coefficients of the first component as

$$\frac{\partial g_1^+(x, y)}{\partial c_{1,k,l}^+} = \beta^3 \left(\frac{x}{s_x} - k \right) \beta^3 \left(\frac{y}{s_y} - l \right) \ . \tag{14}$$

This derivative is the same in the case of the second component.

The derivative of E_{cons}^+ with respect to any of the deformation coefficients of the second component of the direct deformation field is calculated in an analogous way.

Let us see now the derivate of E_{cons}^+ with respect to the coefficients of the first component of the inverse transformation:

$$\frac{\partial E_{\text{cons}}^+}{\partial c_{1,k,l}^-} = -2 \sum_{\mathbf{x} \in \Omega^+} \left(\mathbf{x} - g^-(g^+(\mathbf{x})) \right) \cdot \left(\frac{\partial}{\partial c_{1,k,l}^-} \left(g^-(g^+(\mathbf{x})) \right) \right) \ . \tag{15}$$

Where

$$\frac{\partial}{\partial c_{1,k,l}^+} \left(g^-(g^+(\mathbf{x})) \right) = \frac{\partial}{\partial c_{1,k,l}^+} \left(g^-(x', y') \right) = \beta^3 \left(\frac{x'}{s_x} - k \right) \beta^3 \left(\frac{y'}{s_y} - l \right) \ . \tag{16}$$

The derivative of E_{cons}^+ with respect to any of the deformation coefficients of the second component of the inverse deformation field can be calculated in an analogous way. The derivatives of E_{cons}^- are easily inferred in a similar way. We refer to the original article [11] for the derivatives of E_{img}, E_μ and $(E_{\text{div}} + E_{\text{rot}})$.

3   Choice of w_c

All the energy terms of the functional represent different measurements over the images or the deformations, thus presenting different units. Therefore, the terms are not comparable and a weight term is needed. We determined the optimum value experimentally. While value of zero is useful to compare results with the previous algorithm, weight values around 10.0-30.0 often showed the best compromise between the final similarity and the deformation consistency for our images. Higher values make the consistency constraint too rigid and consequently decrease the images similarity. Lower values cause the lack of relevance between g^+ and g^- in the optimization process and thus do not achieve symmetric transformations. Fig. 1 shows the evolution of the similarity and consistency errors with respect to w_c. The consistency error decreases with the weight but causes a significant increase in the similarity error when approaching to values close to 100. The similarity error is defined as the energy of the difference between the target and the warped source image, while the consistency error is the consistency energy explained above.

For the rest of weight terms we refer to [11]. From our own experience we recommend to set w_i to 1.0 and if necessary, w_μ to 1.0 and w_d and w_r to 0.1.
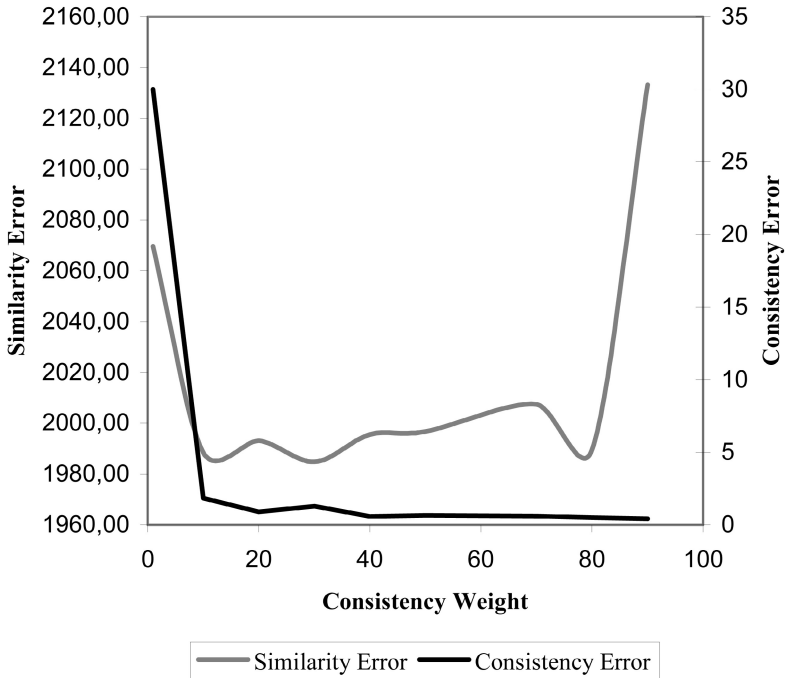
Fig. 1. Evolution of the similarity and consistency error with increasing values of the consistency weight

4   Results

To evaluate our algorithm we tested its performance using synthetic images. We applied some known deformations to the images and then checked whether our method could correct the deformation. That also allowed us to compare our algorithm with the standard one [11]. For instance, in Fig. 2 we have registered a Lena picture with a deformed version of the same image. In this case, the standard method properly registers the deformed image with the original one, but is unable to find the inverse deformation field without using soft landmarks, regularization values and a specific image mask. In the same example, our algorithm finds simultaneously both deformation fields (direct and inverse) using only the similarity term and the consistency term of the energy function.

Fig. 3, 4, and 5 contain a relevant example of the results obtained applying our algorithm compared to the results obtained with the original method (lacking the consistency term) using two consecutive histological sections from breast cancer tissue.

Fig. 4 shows the deformation fields calculated with both methods. It is easy to see how our method guarantees the consistency between the direct and the inverse transformation while the traditional method does not.

Fig. 2. From top to down, left to right: source image, target image, registered source image (by the standard method), registered source image (by our new method), registered target image (by our new method)
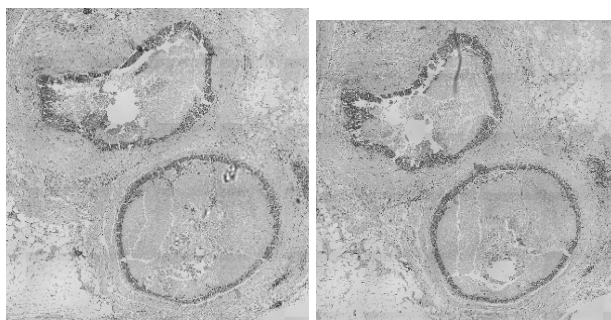

Fig. 3. Two consecutive histological sections from a human biopsy presenting two big tumors

In Fig. 5 we show the result of subtracting the deformed source and target images. We can appreciate how for the inverse transformation our method achieves a much better result than the standard method, as we expected by observing the deformation fields on Fig. 4. These results were also evaluated numerically obtaining an average of similarity error 31.63 of and 32.68 for the deformations calculated with the original method (direct-inverse and inverse-direct) and an average
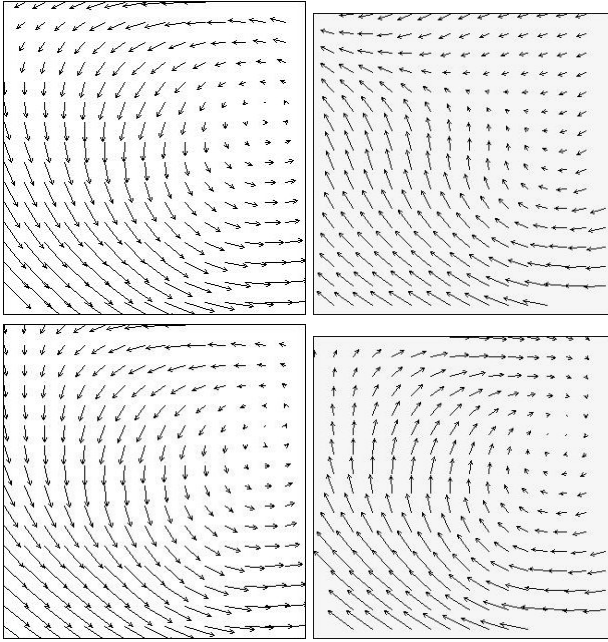
Fig. 4. Comparison of the deformation fields obtained with the original method described in [11] and our new algorithm over the images in Figure 2. The first row shows the deformation when registering image 1 to 2 (left) and image 2 to 1 (right), applying the traditional energy functional. The second row shows the same deformations when using the proposed improvement.

of 31.48 and 31.66 for the deformations of our new method. The differences between the inverse-direct averages provoke visible changes on the registration as shown in the deformation fields representations on Fig. 4.

The gray-scale sample images in Fig. 3 have respectively 325x325 pixels and 300x312 pixels and it took 18 seconds to properly register them in an Intel Pentium M, 1.60 GHz, 589 MHz, 512MB of RAM memory, under a SuSE Linux system.

Fig. 6 is another example with breast tissue sample where the standard method is unable to approach any proper deformation between the source and target images based in the images similarity but where our new method achieves easily the right deformation thanks to the consistency term.

As inferred from the experimental results using our bidirectional method, in most cases only the similarity and the consistency term are needed to achieve a proper registration. This involves a simplification of the energy functional to be minimized and therefore, a reduction in the computational time and complexity. At the same time, forgetting about placing soft landmarks in the images allows us reducing the human interaction in the registration process, which is another advantage of our algorithm over the previous method.
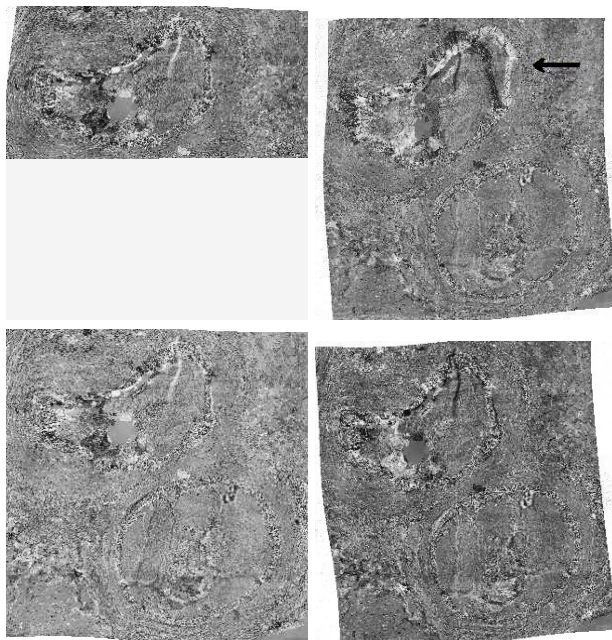
Fig. 5. The top row shows the subtractions of the deformed images and the target ones in both senses, using the traditional method. The bottom row shows the result when applying our method. The black arrow points the most relevant error committed by the standard method.

5   Conclusion and Future Work

A new algorithm for consistent elastic registration has been presented. It combines the ideas of elastic image registration based on B-splines models and consistent image registration. The method improves the results obtained without the consistency factor in the energy function, as it has been qualitative and numerically shown in the results section, and accelerates the search for the optimum. We are aware that a more detailed quantitative evaluation of the algorithm is necessary. This evaluation is currently in progress.

This method can be extended increasing the number of images involved in the registration to do group-wise registration. For this case, the explicit derivatives must be recalculated and a method for composing the deformation fields needs to be proposed.
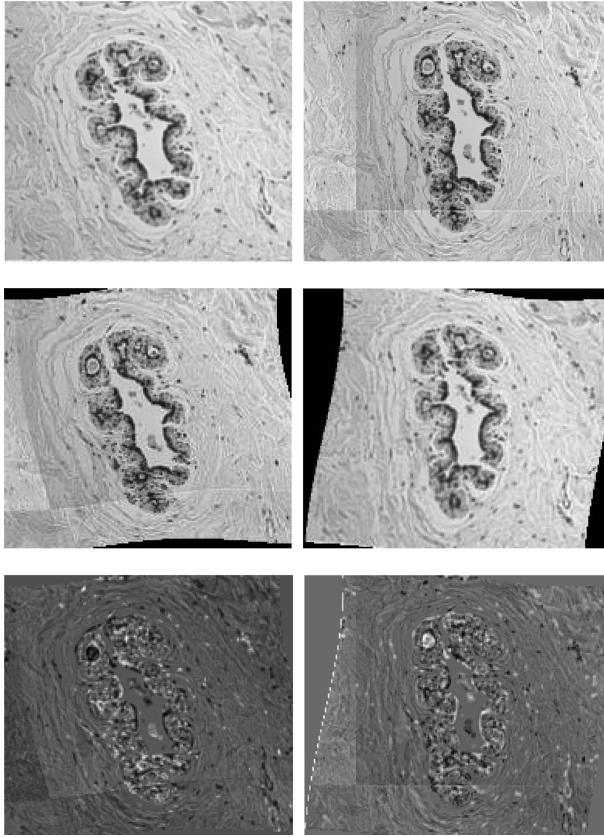
Acknowledgments

Fig. 6. Example with two transversals cuts of a mammary duct. From top to down, left to right: source image, target image, registered target image, registered source image, difference source image, difference target image.

References

1. Fernandez-Gonzalez, R., Jones, A., Garcia-Rodriguez, E., Chen, P.Y., Idica, A., Barcellos-Hoff, M.H. and Ortiz-de-Solorzano, C.: "A System for Combined Three-Dimensional Morphological and Molecular Analysis of Thick Tissue Speciments", Microscope Research and Technique 59(6): 522-530, 2002.

2. Fernandez-Gonzalez, R., Deschamps, T., Idica, A., Malladi, R. and Ortiz-de-Solorzano, C.: "Automatic segmentation of histological structures in mammary gland tissue sections", Journal of Biomedical Optics, vol. 9, pp. 444-453, 2004.
3. Hajnal, J. V., Hill, D. L. G., and Hawkes, D. J.: Eds., Medical image registration, CRC Press, 2001.
4. Maintz, J. B. A. and Viergever, M. A.: "A survey of medical image registration", Medical Image Analysis, vol. 2, no. 1, pp. 1-36, 1998.
5. Arganda-Carreras, I., Fernandez-Gonzalez, R. and Ortiz-de-Solorzano, C.: "Automatic Registration of Serial Mammary Gland Sections", The 26th International Conference of the IEEE Engineering in Medicine and Biology Society (EMBS), 1-5th September, 2004, San Francisco, California.
6. Radeva, P., Amini, A. A., Huang, J.: "Deformable B-Solids and Implicit Snakes for 3D Localization and Tracking of SPAMM MIR Data", Computer Vision and Image Understanding, vol. 66, no. 2, May, pp. 163-178, 1997.
7. Huang, J., Abendschein D., Dávila-Román V. G., Amini, A. A.: "Spatio-Temporal Tracking of Myocardial Deformations with a 4-D B-Spline Model from Tagged MRI", IEEE Transactions on Medical Imaging, vol. 18, no. 10, October 1999.
8. Rueckert, D., Sonoda L. I., Hayes, C., Hill, D. L. G., Leach, M. O., Hawkes D. J.: "Nonrigid Registration Using Free-Form Deformations: Application to Breast MR Images", IEEE Transactions on Medical Imaging, vol. 18, no. 8, August 1999.
9. Christensen, G.E. and He, J.: "Consistent nonlinear elastic image registration", Mathematical Methods in Biomedical Image Analysis, MMBIA 2001, IEEE.
10. Avants, B. B., Schoenemann, P. T., Gee, J. C.: "Lagrangian frame diffeomorphic image registration: Morphometric comparison of human and chimpanzee cortex", Medical Image Analysis (in press).
11. Sorzano, C.O.S., Thévenaz, P. and Unser, M.: "Elastic Registration of Biological Images Using Vector-Spline Regularization", IEEE Transactions on Biomedical Engineering, vol. 52, no. 4, pp. 652-663, April 2005.